Predictor BIST: An "All-in-One" Optical Test Solution for CMOS Image Sensors

Julia Lefèvre, Philippe Debaud, Patrick Girard, Arnaud Virazel

Predictor BIST: An "All-in-One" Optical Test Solution for CMOS Image Sensors

J. Lefevre [1, 2] P. Debaud [1] P. Girard [2] A. Virazel [2]

[1] STMicroelectronics
Imaging division, DFT
Grenoble, France
julia.lefevre@st.com, philippe.debaud@st.com

[2] LIRMM
University of Montpellier / CNRS
Montpellier, France
<lastname>@lirmm.fr

Abstract—The optical test of CMOS Image Sensors (CIS) represents a major part of the overall test time. It consists in applying two-dimensional image processing algorithms on the output images of the CIS under test. In [1], we demonstrated that it is possible to embed 50% of these algorithms in the CIS by using a dedicated Built-In Self-Test (BIST) engine without impacting the defect coverage and at a negligible area cost (approximately 0.25% of the total sensor area). The use of a BIST solution reduces the optical test time by roughly 30% when compared to the optical algorithms traditionally applied by using an Automatic Test Equipment (ATE). However, the effectiveness of this approach is limited by the fact that some global subtle defects cannot be detected. This is a real problem as these defects can seriously impact the output image quality. To overcome this drawback, this paper presents a new BIST solution, called Predictor BIST (PRED BIST) based on a global overview of the image under test. The novelty of this approach lies in the use of an arithmetic method to build an ideal (*i.e.*, predicted) image from wisely selected samples extracted from each output image of the CIS under test. The process of building an ideal image is repeated for all images to be checked for the CIS under test. By comparing each output image to the ideal image, it is then possible to classify good and bad images. Moreover, PRED BIST is an all-in-one test solution that allows to fully replace the optical test done today with an ATE by an embedded test solution. This is an important and unique feature of PRED BIST. Two databases were used to validate this new BIST solution. The first one is an extension of the monocolor database of 27,600 images used in [2] and the second one contains 81,840 images from a RGB sensor. Validation shows that compared to conventional ATE-based test, a correlation of 99.90% and 99.40% respectively is achieved regarding the classification between good and bad images of two considered databases. Moreover, the global defects missed by the test solution in [1] are always found by PRED BIST. This new test solution results in a reduction of up to 95% of the optical test time.

Keywords—CMOS image sensor, BIST, optical test, interpolation.

I. INTRODUCTION

CMOS **I**mage **S**ensors (CISs) are key sensors for the human activities. Rearview camera in cars or camera in smartphones are massively used everyday and they contain CISs. Beside consumer applications, CIS can also be found in industrial (*i.e.*, automotive) or spatial domains.

A CIS converts light information into a machine-readable information [3]. The sensor is built in two parts: electrical and optical. The electrical part contains amplifiers, **A**nalogue to **D**igital **C**onverters (ADCs) and decoders. The decoders access and read the main optical element of the sensor: the pixel array. Inside each pixel (*i.e.*, picture element) of the pixel array, there are transistors and a photoelement.

The conversion flow from the light information (*i.e.*, photons) to the electrical information (*i.e.*, electrical charge) is the following. Once a photon meets the surface of the pixel array, it is converted into an electrical charge thanks to the photoelectric effect induced by the photoelement [4]. The pixel array is read by addressing each row and column. Then, the electrical signal is amplified and converted into a digital bit word to build a digital output image.

However, during the conversion flow, some issues may happen due to defects that can occurred during the manufacturing process. For example, the presence of dust during the manufacturing stage can cause defects (*i.e.*, shorts or opens) between two adjacents electrical rows [4]. To avoid declaring such a defective sensor as good, testing the whole sensor is needed to be sure that its behavior respects the specifications.

The industrial test of a CIS is traditionally performed thanks to an **A**utomatic Test **E**quipement (ATE). The test flow is split into electrical and optical tests to verify all the sensor elements [5]. The major part of the test time is taken by the optical tests. Optical tests consist in putting the sensor in different light conditions, by changing the illumination applied on the sensor, the duration of the photon capture (*i.e.*, integration time) and the gain of the ADC. By doing this, it is possible to verify the sensor behavior in representative conditions. The behavior of the sensor is verified by checking a given number of output images. Optical tests consist in image processing algorithms applied on each selected output image. By using two-**D**imensional (2D) convolution or median filtering, the optical test program running on the ATE is able to compute image quality metrics such as mean of the pixel array, standard deviation, maximum or minimum values, etc. These values are compared to the specifications and if the values are outside the specified range, the corresponding test is tagged as *FAIL* and the sensor is

rejected. Optical tests require precise material (*i.e.*, stable light source) and take a huge amount of data storage (*i.e.*, output images in several conditions and test data). Consequently, conventional external test approaches based on the use of an ATE have a huge impact on the final product cost [6,7].

In [1], we proposed a dedicated **B**uilt-**I**n **S**elf-**T**est (BIST) engine to reduce the optical test time that takes the major part of the test time as mentioned previously. This BIST solution, called **P**ixel **E**mbedded **T**est **S**olution (PETS), is a local test solution to verify the pixel values. It works in one-**D**imension (1D), at-speed (*i.e.*, clocked at the pixel reading speed) and it does not require to store all entire images as for ATE-based optical tests. To validate PETS BIST, experiments were done on **D**ata**B**ases (DBs) containing output images coming from two different monocolor (grayscale) sensors, the first one composed of 4,800 images (DB1) and the second one composed of 27,600 images (DB2). The *correlation* was used to validate the efficiency of PETS BIST and is defined as the percentage of correspondence between the classification of good/bad images given by the ATE-based optical tests and the one given by PETS BIST. The correlation was found to be 99.95% and 99.64% for DB1 and DB2, respectively. For the considered DBs, PETS BIST represents only 1% of the digital part of the sensor, *i.e.* 0.25% of the total CIS area. By studying the optical algorithms applied with the ATE, we calculated that roughly 50% of the optical tests can be covered by PETS BIST. This represents a reduction of 30% of the overall optical test time.

PETS BIST partially reuses the traditional way of testing CISs–- as usually performed with an ATE–- and has good correlations with ATE-based optical tests results. However, the results on DB1 and DB2 showed that some subtle global defects, such as defective columns, are sometimes missed. More precisely, the difference between PETS BIST-based results and ATE-based results represents 0.36% of DB2, with 0.28% due to defective columns that are missed by PETS BIST.

In this paper, a new test solution, called **PRE**dictor (PRED) BIST, is proposed to alleviate this issue. Moreover, PRED BIST is an all-in-one test solution that allows to fully replace the optical test done today with an ATE by an embedded BIST solution. This is an important and unique feature of PRED BIST. It builds an ideal image from samples selected inside the image under test. An offset is added to the pixel values of the ideal image to create an admissible envelope around the image under test. Finally, PRED BIST sorts correct and defective pixels by comparison between the envelope and the image under test: if a pixel value of the image under test is outside the envelope, the pixel is tagged as defective. PRED BIST validation has been done thanks to an extended version of DB2 (45,800 images for PRED BIST validation versus 27,600 for PETS BIST validation) and thanks to 81,840 images from **R**ed-**G**reen-**B**lue (RGB) sensors (DB3). The correlation was found to be 99.90% and 99.40% for DB2 and DB3, respectively. For the considered DBs, PRED BIST represents 1.5% of the total CIS area. All of the optical tests are covered by embedding PRED BIST to perform the optical tests inside the CIS. This induces a reduction of 95% of the overall optical test time. This estimation results from the study, during the test flow, of how many optical algorithms are covered by the PRED BIST usage.

The paper is organized in five main parts. Section II deals with the background of the study by providing information on what is a CIS and how CISs are tested today. Section III summarizes the previous work done in [1] and [2]. Section IV details our proposed innovative PRED BIST solution. Section V presents the results achieved by using PRED BIST. Section VI discusses the advantages of the proposed PRED BIST solution compared to PETS BIST presented in [1]. Section VII concludes the paper.

II. Background

A. CMOS Image Sensor Overview

A CIS contains electrical and optical blocks. The main optical block is a pixel array. Each pixel of the pixel array contains a photoelement, generally a photodiode which converts the photons into electrons owing to the photoelectric effect [4]. Several pixel architectures exist, the difference between the architectures being the presence of a more or less complex readout circuitry. This readout circuitry can contain a reset transistor, an amplifier, a row select transistor, etc [8].

The pixel array is covered by an array of microlenses to focus the light rays on the photelement inside each pixel to avoid loosing light information.

Row and column decoders are part of the electrical blocks. They are driven by a sequencer block and they are used to stream the pixel array to address each pixel horizontally, *i.e.* row by row, at the pixel clock rate (*i.e.* , pixel reading speed). The electrical charges from the pixels pass through column amplifiers before to be converted to a digital bit word by an ADC. The digital image can then be modified thanks to the **I**mage **S**ignal **P**rocessor (ISP) to do some calibration or noise filtering. Note that the ISP is independent from the **C**entral **P**rocessing **U**nit (CPU) of the system and is only used to perform operations on output images of the CIS.

The digital pixel value depends on the quantity of the captured photons. If a large amount of photons is collected, the pixel value is higher than if there is only few photons. This is also relative to the **Q**uantum **E**fficiency (QE) of the photoelement, which is the number of created charges versus the number of incident photons. The information given above is illustrated in Fig. 1. The pixel value is encoded on N bits, allowing to quantify the intensity of the incoming light.

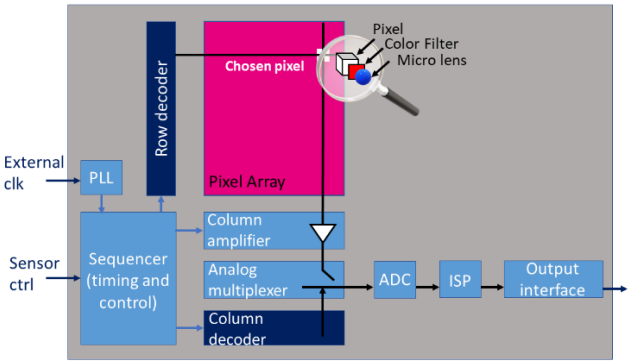

Figure 1: General architecture of a CMOS Image Sensor

Between the pixel array and the microlens array, a **C**olor **F**ilter **A**rray (CFA) can be inserted to give to each pixel a color information. The most common CFA is the Bayer color filter organized in a 2x2 Kernel of pixels (Red/Green1 on the

first row and Green2/Blue on the second row) [9]. The Green information is duplicated compared to the red and blue ones to mimic the human eye. Depending on the presence or the absence of the CFA, a sensor can be characterized as RGB or monocolor. Using a RGB or a monocolor CIS depends on the final application of the sensor.

B. State-of-the-Art in CIS Testing

The test of a CIS is usually performed with an ATE and the resulting data is saved into a **S**tandard **T**est **D**ata **F**ormat (STDF) file [10]. The STDF file can be used later for diagnosis purpose in production. For RGB CIS, the test information of each color channel can be accessed independently inside the STDF file. During the test process, if one test fails, the sensor is considered as defective. The CIS test flow is split into electrical and optical tests to verify the whole architecture presented in Fig. 1. Electrical tests can be parametric, functional or structural depending on the part of the circuit under test (*i.e.*, analog, digital or mix). They consist in applying test stimuli at the inputs of the circuit and verify that the outputs meet the expected specifications (*i.e.*, correct parameters, correct function, …). Electrical tests take much less time than the optical ones [7].

Optical tests rely on the storage inside a memory of several output images of the CIS under test. The number of images to save depends on the CIS under test and on the test program. The distribution of the output images is depicted in Fig. 2. The operation of a CIS highly depends on the illumination. The input or sensitisation part of the CIS is the incoming light whereas the output or observation part is the pixel value. Therefore, by varying several conditions (type of illumination, integration time or ADC gain), the optical test allows to put the sensor in several states and to verify its correct operation in a wide variety of conditions. The illumination condition can lead to Dark or Light images, coming from no-light and light conditions respectively [13].

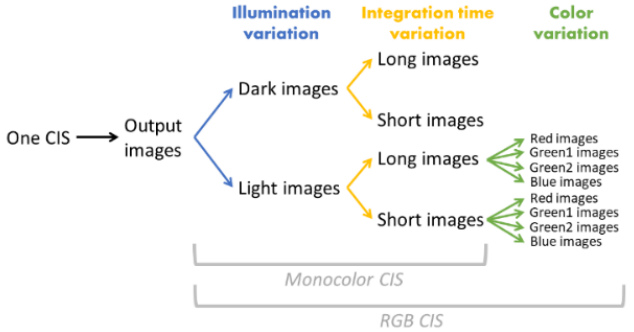

Figure 2: Distribution of the output images from one CIS (monocolor or RGB) [2]

For some CISs, the presence of a lens between the light source and the sensor is necessary. This feature results in a non-uniformity inside the Light image where the pixel values at the center of the image are higher compared to the pixel values at the borders of the image. In a fault-free case, the arrangement of the pixel values in the Light image has a Gaussian shape whereas the Dark image is uniform (*i.e.*, constant). In the case of a RGB CIS, Light images can be split into Red, Green1, Green2 and Blue color images. To split Light images, pixels of the same color are joined together inside a new image with a lower size than the original one. The integration time is the duration between the beginning and the end of the photon capture [11,12]. It can be a Short or a Long integration time, inducing a bigger sensitivity to noise in the Short case.

The notation used to refer to one specific output image is to join the illumination, integration time and color denominations. For example, an image taken in the light illumination, with a short integration time and on the Red color channel, will be called a Light Short Red image (Fig.2).

During optical test, it is mandatory to wait for the output images (*i.e.*, four output images for monocolor CIS and ten output images for RGB CIS) to be saved into a memory before launching the optical algorithms on these images. The optical algorithms are 2D image processing algorithms like, for example, convolution processing, median filtering or other basic image processing techniques [5]. These tests are applied to detect potential optical defects (*cf.* Section III.A. for defect definition) and to compute image quality metrics such as noise level inside the image. Finally, the quality metrics determine if the output image is good or not.

A label (*PASS* or *FAIL*) is used to know the state of the output image. The image label (also called STDF label for ATE-based optical tests or BIST label for BIST-based tests) is set for the output image at the end of the optical tests. The label of the sensor is the compilation of labels of its output images. The term “compilation” depicts the fact that if all output image labels are *PASS* (*i.e.*, meaning that all optical tests have passed on all output images), the sensor label will be *PASS*, but if only one output image label is *FAIL* (*i.e.*, at least one optical test has failed on at least one output image), the sensor label will be *FAIL* and the sensor will be rejected. Several compilations are done to have the label of the sensor: a compilation at color channels level (*i.e.*, Red, Green1, Green2 and Blue labels compilation for Light images), a compilation at integration time level for each illumination condition (*i.e.*, Light Long/Light Short labels compilation and Dark Long/Dark Short labels compilation) and a compilation at illumination conditions level (*i.e.*, Light/Dark labels compilation). At each level of the compilation, an intermediate label is assigned.

III. Previous Work

A. Defect Definition

Optical tests detect defects by applying several optical algorithms on the output images of the CIS under test. Each optical algorithm targets a specific category of defects inside the CIS under test. Sometimes a defect inside the optical part of the CIS does not cause any visible issue inside the output image. But if it does, one of the optical algorithms must find it, generally by looking for a break in the homogeneity of the image.

A defect is a deviation from the specification. A certain pixel value is expected in precise conditions (*i.e.*, illumination, integration time or ADC gain). Nevertheless, a range around the admissible pixel value (more or less a few gap) is allowed due to the presence of noise. The pixel value which is too distant from the expected value is defined as a defective pixel. The notation used to refer to the defective pixels is the following: if the pixel value is ‘0’ (or near to ‘0’), the pixel is considered as a *dead* pixel. If the pixel value is the maximum pixel value, it is a *hot* pixel, and if the value differs too much compared to the correct value, it is a *weak* pixel.

A defective image is recognizable by the difference of pixel values inside the image compared to the value of a correct pixel. For example, a group of defective pixels can be found if several pixels in the same area are impacted by the defect. This kind of defect is called a local defect. Some examples of local defects are depicted in Fig. 3.

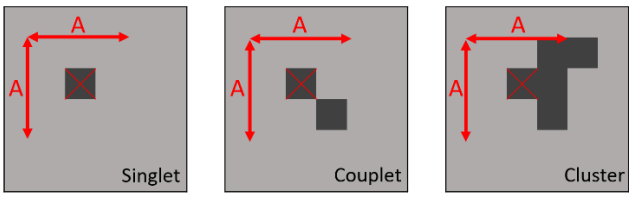

Figure 3: Examples of possible local image defects [14]

In this paper, we consider three categories of local defects. The local defects are defined in a 2D A*A kernel of pixels, containing A^2 pixels. A is an odd integer which depends on the size of the pixel array, so it depends on the CIS under test. These definitions are valid only if the pixel at the middle of the A*A kernel of pixels is defective. One defective pixel in the middle of an A*A kernel of pixels is defined as a *singlet*, two defective pixels are a *couplet*, and more than two defective pixels is defined as a *cluster*. The STDF file can contain more categories of defects such as triplet (*i.e.*, three defective pixels in the A*A kernel) or quadruplet (*i.e.*, four defective pixels in the A*A kernel) for diagnosis purposes. The proposed BIST solutions only use the three categories depicted in Fig. 3 by considering that a triplet or a quadruplet are particular cases of cluster and that the presence of these defects is a key element to reject a CIS. This choice has been done because PRED BIST is used for testing CIS and not for diagnosis.

Admissible limits are defined for each category of local defects. The limit for singlets is not the same than the limit for couplets because the incidence on the output image quality is not the same. If a cluster is found inside the pixel array, the label of the image is defined as *FAIL*, and the sensor is rejected because a cluster will seriously compromise the quality of the output image.

Other defects, such as row or column of defective pixels which can be seen as particular cases of cluster, high noise or wave (*i.e.*, diagonal distribution of the difference of pixel values inside the image) can be present in a defective image. These kinds of defect are global defects. Figure 4 illustrates some examples of global defects.

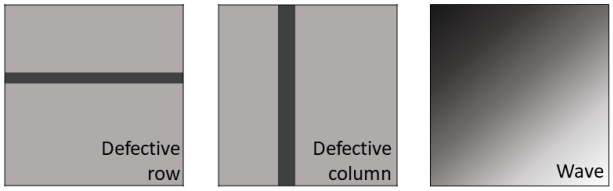

Figure 4: Examples of possible global image defects [14]

There is no admissible limit for global defects. If a global defect is found inside the image of the CIS under test, the label of the image is *FAIL* and the sensor is rejected.

B. PETS BIST Solution

The motivation of the work presented in [1] and [2] lies in the fact that the optical test cost, when performed by an ATE, is high in terms of memory usage and test application time due to the storage of the output images and the 2D image processing algorithms.

PETS BIST is a digital solution that aims at reducing the optical test time. This test solution is split into hardware and software parts to perform a functional test of the optical elements of the CIS under test. The input of PETS BIST is the digital pixel values coming from the pixel array. Therefore, the BIST structure is physically located next to the pixel array inside the sensor, directly after the ADC, to receive the pixel values without any treatment that can occur in the ISP.

The general architecture of PETS BIST is depicted in Fig. 5. The hardware part, in the grey rectangle in Fig. 5, is the core of PETS BIST whereas the blocks outside the grey rectangle are parts of the system and perform operations like bus communication, control, etc.

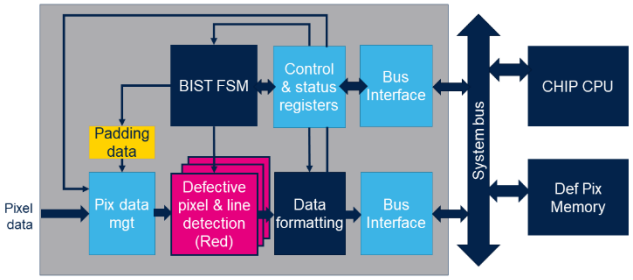

Figure 5: General PETS BIST Architecture [1]

The hardware part contains several blocks and each block performs a dedicated function [1]. It is used to detect all the defective pixels inside the pixel array and saves the data into an external memory, called *Defective Pixel Memory* ("Def Pix Memory" block in Fig. 5). The process of defective pixel detection is the following. The pixels of the pixel array are streamed thanks to row and column decoders at the pixel clock rate. The *Pixel Data Management* block ("Pix data mgt" block) guides the **P**ixel **U**nder **T**est (PUT, the current addressed pixel value) in the dedicated accumulator inside the *Defective Pixel and Line Detection* block to deal with the PUT with pixels of the same type (Red, Green1, Green2, Blue or monocolor). A local average of the four nearest neighboring pixel values of the PUT (on the same row) is computed inside the *Defective Pixel and Line Detection* block. The local average is computed in 1D thanks to a 1*5 array of pixels by excluding the PUT value at the center. An admissible range (*i.e.*, in which the pixel value is correct), composed of a low and a high thresholds (Thr_{min} and Thr_{max} respectively), is computed from the local average. The definitions of the two thresholds are given in Eq. 1 and are valid for all the conditions (i.e., different illuminations, integration times and ADC gains). This genericity relies on the settings of a percentage of the local average (thanks to a_{min} and a_{max}) and the addition of offsets (thanks to b_{min} and b_{max}) to create the most precise range depending on the conditions. The calibration of the constants has been done by comparison between the number of defective pixels in the STDF file and the number of defective pixels found by PETS BIST [2].

$$\begin{cases} Thr_{min} = a_{min} \times local_{average} + b_{min} \\ Thr_{max} = a_{max} \times local_{average} + b_{max} \end{cases} \quad (1)$$

If the PUT value is outside the range $[Thr_{min}; Thr_{max}]$, the PUT data is formatted by the *Data Formatting* block and

is stored in the *Defective Pixel Memory* (for diagnosis purpose). The saved data is the type of the pixel, the pixel value and the coordinates of the defective pixel relative to the pixel array.

The software part, a C code embedded on the chip CPU of the sensor, read the *Defective Pixel Memory* and classifies the defective pixels into singlet, couplet or cluster categories. From the categories definition, the software part determines if the image under test is good or bad by comparing the admissible limits of each category to the computed number of defects of each category. If the image is bad, the sensor is rejected.

PETS BIST has been implemented in Verilog language. The estimated size of PETS BIST was computed in terms of additional logic gates. PETS BIST is made of about 1k Flip-Flops and represents an addition of only 0.25% of the total area for a 1.5 MegaPixels sensor.

The validation of PETS BIST has been done thanks to two different DBs of 4,800 images (DB1) and 27,600 images (DB2). These images come from two different monocolor sensors. With the correct constants settings of the BIST (*cf.* [2]), the correlations between ATE-based optical tests results and PETS BIST results are 99.95% and 99.64% respectively. The correlation depends on the comparison between the label from the STDF file and the label from PETS BIST for each image in the DB. If the STDF label is *PASS* then PETS BIST should not find any optical defect inside the output image. Conversely, if the STDF label is *FAIL*, PETS BIST needs to find a cluster or a number of singlets (or couplets) that are outside the admissible limits. The differences of 0.05% and 0.36% for the two DBs show that PETS BIST misclassifies images with a *FAIL* label by putting a *PASS* label on it. By looking at the cause of the misclassification, it was shown that 80% of the misclassified images are images with a defective column. In all cases, the missed defective column is a column composed of pixels with a slight difference compared to the pixel values in the adjacent columns. Missing such a defect is prohibited because a defective column highly influences the quality of the image.

The BIST insertion still requires the use of the ATE-based optical tests to cover the global defect detection. PETS BIST can embed approximately 50% of the optical algorithms, thus saving about 30% of the optical test time when compared to a test fully performed with an ATE. This estimation results from the study, during the test flow, of how many optical algorithms are covered by the PETS BIST usage.

IV. Proposed Predictor BIST Solution

A. Principle of the Proposed Test Approach

The human eye is very sensitive to global variations. For example, a "huge" defect inside an image (*i.e.*, a defect affecting a significant group of pixels) will easily be found while a single defective pixel will not be. A human considers the homogeneity of the entire image as a key point to decide if it is a good or a bad image.

The proposed test solution, called PRED BIST, is a digital BIST solution that still has the same objective as PETS BIST, *i.e.*, to reduce the optical test time. Its main difference is based on a global overview of the image (as a human would do), which handles an image as a continuous mesh of pixel values.

By adopting the same architectural organization as PETS BIST, PRED BIST is split into hardware and software parts. The hardware part, embedded inside the CIS, detects all the defective pixels, and the software part classifies them. The software part of PRED BIST reuses the C code from PETS BIST to perform the classification.

Operating PRED BIST is done in several phases that require to read the pixel array twice: a first time to read and select samples inside the image (called phase 1 in the following), and a second one to build the ideal image and to compare the ideal and the real images (phase 2 and 3 simultaneously). PRED BIST computes an ideal image from each output image of the CIS under test owing to an arithmetic method (*i.e.*, bilinear interpolation). The ideal image is then compared to the real image. Offsets are added to the ideal image to perform the comparison since, during the real CIS operation, the image never totally matches the ideal image. These offsets create a range defining the correct pixel values.

PRED BIST detects all global defects (*i.e.*, defective row or column, noise presence, etc.) and is also able to catch local defects such as singlets, couplets, etc. Unlike PETS BIST that still requires the use of an external test to detect global defects, **all** optical algorithms usually applied by an ATE are covered by the use of PRED BIST, making this solution an "all-in-one" test solution. It results in a reduction of up to 95% of the optical test time. Moreover, PRED BIST avoids the storage of full images as it only needs to save few pixel values inside the image.

B. Phase 1: Selection of Reference Points

The first phase is an initialization phase. The pixel array is streamed row by row at the pixel rate thanks to the sequencer block (*cf.* Section II.A.). During the reading, the pixel array is divided into 5*5 rectangular sub-arrays. A reference point is selected at each intersection of the 25 sub-arrays.

At the end of this first phase, the 25 reference point data (pixel values and coordinates) is saved into an external memory, called *Reference Points Memory* in the following. Note that the ideal image is not saved entirely, only the reference points are saved into the *Reference Points Memory*.

C. Phase 2: Prediction of the Ideal Image

After the initialization of the reference points done in Phase 1, Phase 2 exploits data in the *Reference Points Memory*. The ideal image is built, with the same size as the real image, by filling the blank between the reference points thanks to a bilinear interpolation.

$$f(x_a, y_a) = f(x_1, y_a) * \left(\frac{x_a - x_1}{x_2 - x_1}\right) + f(x_2, y_a) * \left(\frac{x_2 - x_a}{x_2 - x_1}\right)$$

with (2)

$$\begin{cases} f(x_1, y_a) = f(x_1, y_1) * \left(\frac{y_a - y_1}{y_2 - y_1}\right) + f(x_1, y_2) * \left(\frac{y_2 - y_a}{y_2 - y_1}\right) \\ f(x_2, y_a) = f(x_2, y_1) * \left(\frac{y_a - y_1}{y_2 - y_1}\right) + f(x_2, y_2) * \left(\frac{y_2 - y_a}{y_2 - y_1}\right) \end{cases}$$

Equations 2 are used to build the ideal image and are illustrated in Fig. 6. x and y are the coordinates (integer type) relative to the rows and columns of the pixel array. $f(x_a, y_a)$ is the pixel value of point A with the coordinates (x_a, y_a).

The reference points are depicted in dark blue in Fig. 6 and are denoted as A_{11}, A_{12}, A_{21} and A_{22}. These four reference points define one plan of reference. The values of the intermediate points A_{1A} and A_{2A} are built from the values of the reference points. The bilinear interpolation from Eq. 2 is used to build the value of point A of coordinates (x_a, y_a) ($x_1<x_a<x_2$ and $y_1<y_a<y_2$) from the values of points A_{1A} and A_{2A}.

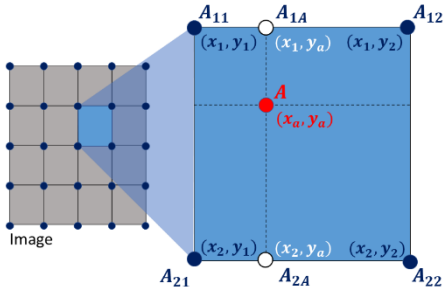

*Figure 6: Bilinear interpolation for point A (x_a, y_a) inside the image for 5*5 reference points*

The same process using the bilinear interpolation from Eq. 2 is performed for each pixel value inside all the plans of reference in Fig. 6. These ideal (interpolated) values computed from the values of the real image are represented in Fig. 7.a.

The ideal image in Fig. 7.b, is composed of 16 contiguous plans of reference computed from the 25 reference points selected inside the real image in Fig.7.a, thanks to the bilinear interpolation from Eq. 2.

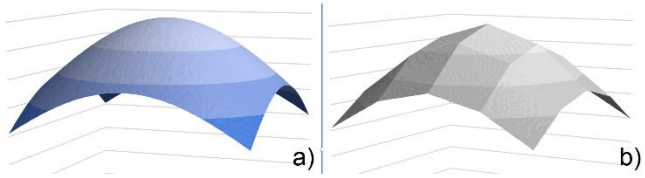

Figure 7: 3D representation of the real image (a) and the ideal image (b)

Note that for the visual representation, the real image in Fig. 7.a is a theoretical image of resolution 100*100 pixels computed from the equation of the gaussian function in 2D [15]. This image is only used to explain the PRED BIST operation. Results presented at the end of this paper have been achieved by using real images captured during the industrial optical test of real sensors.

D. Phase 3: Computation of the Envelope

As mentioned previously, the interpolation will not totally match the real image. An admissible envelope needs to be computed to compare the real and the ideal images. Figure 8 shows the 3D representation of the admissible envelope.

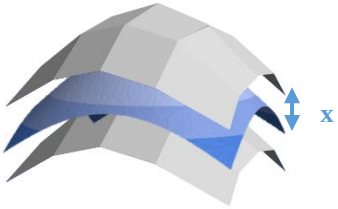

Figure 8: 3D representation of the real image in blue and the envelope in grey computed from the ideal image

The envelope is obtained by using two copies of the ideal image, shifted of x percentage above and bellow the real image. If a pixel value of the real image is outside the envelope, the pixel is defective. The choice of x is critical to calibrate PRED BIST since it defines the thickness of the envelope and so the number of defective pixels. As mentioned previously in Section III.A, the number of defective pixels (and so the number of singlets, couplets and cluster) determines the classification of the sensor (*PASS*/*FAIL*).

E. Architecture of PRED BIST

The CIS die sorting is done by resorting to two types of resources: i) the BIST infrastructure embedded in the CIS for test and defective pixel detection, and ii) two external memories for test data storage. This distribution of tasks has been decided to achieve the best trade-off between test time efficiency and CIS hardware overhead. The CHIP CPU is used for defect classification. One important point is the location of the BIST module inside the CIS architecture. In order to avoid pre-processing on pixel values by the ISP, that could potentially correct and hide potential defects, pixel values must come directly from the pixel array without going through intermediate hardware modules like correction modules, filtering block, scaler block, etc. [16]. The general BIST architecture is depicted in Fig. 9 where each digital block is dedicated to one function. This solution has been implemented in Verilog language.

In order to test all pixels in a CIS array, each pixel is selected based on its type (Red, Green1, Green2, Blue or monocolor) since a pixel of one type can only be tagged as defective with respect to pixels of the same type. The block *Pixel data management* ("Pix data mgt" block in Fig. 9) allows to select the pixels of the same color using to the coordinates of the current pixel.

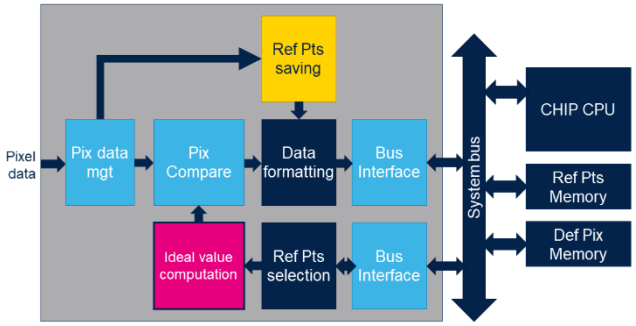

Figure 9: General PRED BIST Architecture

During Phase 1 (*i.e.*, Selection of Reference Points), the pixel array is streamed and the *Reference Points saving* block ("Ref Pts saving") selects all the reference points. The data of the reference points (*i.e.*, pixel values and coordinates) is saved into the *Reference Points Memory* ("Ref Pts Memory"). The pixel array is streamed again and the *Reference Points Memory* is accessed by the *Reference Points Selection* block ("Ref Pts selection") in order to get back the four corresponding reference points thanks to the coordinates of the PUT (x_a, y_a). The values of the four reference points are used to compute the ideal value of the PUT by the *Ideal Value Computation* block (Phase 2). Then, the *Pixel Compare* block builds the envelope and makes a comparison between the real value and the envelope (Phase 3). If the pixel value is outside the envelope, the data of the pixel is formatted by the *Data Formatting* block and saved into the *Defective Pixel*

Memory (“Def Pix Memory”). This memory will be read by a program embedded on the Chip CPU to classify the defective pixels into singlets, couplets or cluster. The program is also able to give a *PASS*/*FAIL* information from the number of defects.

A preliminary study of the PRED BIST architecture in terms of additional logic gates shows that its area represents 1.5% of the total area for a 1.5 MegaPixels sensor.

V. Experimental Results

In order to validate the proposed PRED BIST solution, we performed experiments by using two DBs composed of images taken from CISs in Dark and Light illuminations for Short and Long integration times. The output of the PRED BIST engine is a *PASS*/*FAIL* information related to the CIS under test as well as the number of singlets, couplets and clusters associated to each image. The goal of our experiments is to demonstrate the efficiency of PRED BIST in reproducing the optical tests for CIS as they are usually applied with an ATE, without the drawbacks of long-time duration and huge amount of data storage. Moreover, we show that PRED BIST is a generic test solution which is usable for any CIS regardless of its architecture, size and technology.

A. Experimental Setup

A first DB, called DB2 from the notation used in [2], composed of output images coming from more than 11,450 monocolor CISs originating from different packets, were used in our experiments. Each packet is a set of sensors that have been manufactured on the same production chain. An extract of this DB was previously used to validate PETS BIST [2]. Among these 11,450 CISs, a part of them were identified as *FAIL* by former ATE-based optical tests. Images coming from these CISs were selected so as to get a representative sample of various defect categories, *i.e.*, singlets, couplets, defective columns, defective rows, clusters of various sizes, etc. For each CIS, we collected the same number of Dark and Light images so that the dataset was split into two equivalent sets of Dark (Short and Long) and Light (Short and Long) images as shown in Fig. 10.

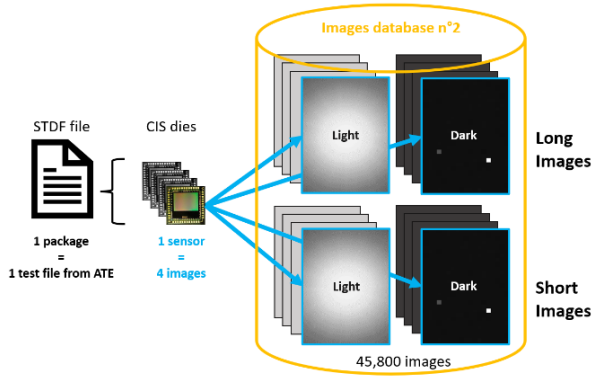

Figure 10: Data distribution of DB2

A second DB, called DB3, is composed of output images coming from 20,460 RGB CISs and is illustrated in Fig. 11. One CIS gives 10 images if the Light image is split into Red, Green1, Green2 and Blue images (*cf.* Section II.B).

The sensors used to build DB2 and DB3 come from different packets of sensors. By this way, a significant number of sensors from different manufacturing conditions can be considered in our experiments. In fact, all the production chains used during manufacturing stage are different due to potential process deviations or difference of settings. Experimental results presented bellow consider each DB as a unique set of sensor images coming from the sum of all the packets.

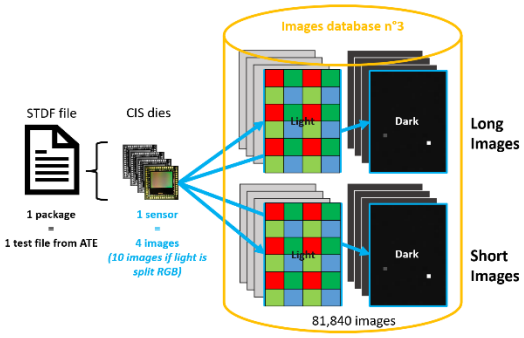

Figure 11: Data distribution of DB3

The subset of images coming from *FAIL* CISs was organized into several categories with respect to the defect type. For each image, the number of singlets and couplets is known, as well as the presence of clusters (*i.e.*, group of defective pixels, defective rows or columns, wave, etc.), thanks to the output data from former ATE-based optical tests (data available into STDF files).

Moreover, we have to calibrate the x parameter used to set the envelope (cf. sub-section IV.D) for each type of sensor (*i.e.*, monocolor or RGB). The x parameters have been selected experimentally to achieve the best trade-off between the admissible number of defective pixels inside all images and the minimization of the number of misclassified images compared to the ATE-based optical tests. The x parameters are calibrated separately depending on DB2 and DB3.

The following sub-sections V.B and V.C explain experimental results obtained after application of PRED BIST for the optical test of sensors providing images in DB3. Results of PRED BIST application on DB2 are detailed in Section V.D and will be discussed and compared with the PETS BIST application on DB2 in Section VI.

The interpretation of the experimental results detailed in the next sub-sections is based on the study of the correlation. As mentioned previously, the correlation is a high level information that quantifies the similarities between the ATE-based optical tests and BIST-based tests. The correlation is achieved by comparing the STDF label and the BIST label of the different groups of image types (*i.e.*, color, integration time and illumination conditions).

To get the STDF label and BIST label of the sensor, there is a need to compile them. The compilation is done sequentially by compiling i) the four labels of the color images, ii) the two labels of the integration time images and iii) the two labels of the illumination condition images. Figure 11 illustrates the compilation process where each arrow corresponds to a compilation.

The label after the compilation at color level (called color compilation in the following) can be different compared to the label after the compilation at illumination level (called “Dark-Light compilation” in the following). For example, if an image has a *PASS* label after the color compilation, nothing prevents it to have a *FAIL* label at the end of all the compilations as a defect in one condition may not be seen in

another condition. This may result in a misclassification of this image (and so the sensor) if all the compilations are not done. The compilations are done for STDF labels and for BIST labels separetely.

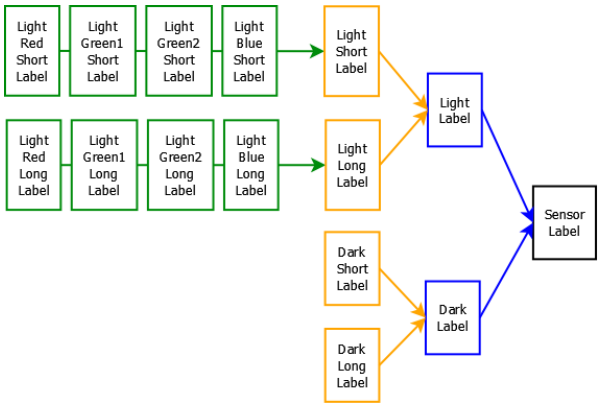

Figure 12: Algorithm view of the compilation process to achieve the sensor label

B. Using PRED BIST for DB3 optical test

The correlations between ATE-based optical tests results and PRED BIST results are given in Tables I, II and III for different levels of compilation (*i.e.*, color, integration time and illumination). These correlations are expressed in percentage and come from the comparison between the STDF label and the PRED BIST label at each level of the compilation process.

Table I shows the correlations before and after the color compilation. The first four rows of Table I deal with the color compilation for Light Short images and the last four rows with the color compilation for Light Long images. The first column gives the image type, the second one gives the correlations for each color image and the third one gives the correlations after the color compilation (Light Short and Light Long correlations). More precisely, the second column gives the correlations of each color channel independently.

TABLE I. CORRELATION BEFORE AND AFTER COLOR COMPILATION FOR LIGHT IMAGES FOR DB3

Image type	Correlation before color compilation (%)	Correlation after color compilation (%)
Light Short Red	99.30	98.02
Light Short Green1	99.75	
Light Short Green2	99.65	
Light Short Blue	98.76	
Light Long Red	99.57	98.81
Light Long Green1	99.80	
Light Long Green2	99.75	
Light Long Blue	99.39	

The correlations of the Light Short Blue and Light Long Blue images are the lowest of all with 98.76% and 99.39%, respectively. The human eye is less sensitive to the Blue color than to the Green or Red ones and the Blue resin used to build the Blue color inside the color filter is more sensitive to noise [17]. The noise induces a difficulty for PRED BIST to match the Blue images, so the correlation is degraded between ATE-based classification and BIST-based classification of the Blue images.

The correlations decreases from before to after the color compilation for Short and Long images. For example, the correlation for Light Short Red images is 99.30%. After the color compilation, the correlation for Light Short images is 98.02%. The decrease is about 0.74% for Short images and 0.58% for Long images compared to the lowest bound of the ranges of color correlations, [98.76%; 99.75%] for Short and [99.39%; 99.80%] for Long. So, the images are more easily misclassified by PRED BIST after the color compilation (*i.e.*, *PASS* images of a given color beeing classified as *FAIL* or *FAIL* images of a given color beeing classified as *PASS* by PRED BIST). It is important to notice that the STDF label of one color is independent to the label of another one, even if the color images come from the same Light image.

The second level of compilation is the integration time compilation. Table II provides the correlation from the two integration time compilations.

The compilation Dark Short/Dark Long is presented on the two first rows and the compilation Light Short/Light Long is presented on the two last rows of Table II. The third column of the table presents the two correlations after the integration time compilation.

TABLE II. CORRELATION BEFORE AND AFTER INTEGRATION TIME COMPILATION FOR DB3

Image type	Correlation before integration time compilation (%)	Correlation after integration time compilation (%)
Dark Short	99.75	99.41
Dark Long	99.65	
Light Short	98.02	98.01
Light Long	98.81	

The compilation at integration time level still has an impact that decreases the correlation in comparison between before and after the integration time compilation. This can be explained by a reasoning similar to the one done for the color compilation presented above, *i.e.*, at this compilation level, PRED BIST can still give a *PASS* label to some images with a *FAIL* STDF label, thus leading to a misclassification of the image.

The third and last level of compilation is the Dark-Light compilation. The correlations for Dark-Light images are given in Table III.

TABLE III. CORRELATION BEFORE AND AFTER DARK-LIGHT COMPILATION FOR DB3

Image type	Correlation before Dark-Light compilation (%)	Correlation after Dark-Light compilation (%)
Dark	99.41	99.40
Light	98.01	

The correlation for Dark images is higher (+1.40%) than the correlation for Light images because Dark images are easier to model with the bilinear interpolation due to the uniformity of Dark images (*cf.* Section II.B.). Thus, the choice of the x parameter for Dark images is less critical than the one for Light images.

After the Dark-Light compilation, 99.40% correlation is reached among PRED BIST-based and ATE-based classifications between *PASS*/*FAIL* images. The

misclassified images in Dark may be well classified in Light (or vice-versa). If the PRED BIST label for an image '*i'* in the Dark is *PASS* and the PRED BIST label for the same image 'i' in the Light is *FAIL*, the label of 'i' after the Dark-Light compilation is *FAIL*.

C. Mismatches analysis of PRED BIST usage for DB3 optical test

After the Dark-Light compilation, it remains few misclassified images (*i.e.*, only 0.60% as reported in Table III). The distribution of the misclassification causes are depicted in the piechart in Fig. 13. The notations are the following. On one hand, the coupMiss, tripMiss and clusMiss causes refer to defects (*i.e.*, couplet, triplet and cluster, respectively) that are missed by PRED BIST during the test. On another hand, the misclassification causes coupOnly and clusOnly refer to defects (*i.e.*, couplet and cluster) that are detected by the PRED BIST engine and not by ATE-based optical tests. The tripOnly cause (*i.e.*, triplets found in excess by PRED BIST) does not exist since, as mentioned previously, the defect categories of PRED BIST are only singlet, couplet and cluster (*cf.* Section III.A.). For couplets, the misclassification causes coupMiss and coupOnly induce the fact that PRED BIST finds a number of couplets which is bellow or above the admissible couplet limit respectively.

PRED BIST nearly always finds the same number of singlets than in the STDF file thus explaining why the singlet cause of misclassification is not present in the piechart in Fig.13. If the number of singlets is above the admissible limit, statistically, there is more chance to create a group of defective pixels, so the misclassification cause will no longer be due to a high number of singlets but a group of defective pixels (couplet or cluster).

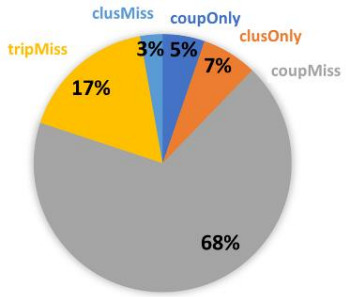

Figure 13: Distribution of misclassification causes after Dark-Light compilation for DB3

The misclassification causes are split into missed defects, which represent 88% of the misclassifications (coupMiss 68%, tripMiss 17% and clusMiss 3%), and defects found in excess (*i.e.*, defects found by PRED BIST and not by ATE-based optical tests, coupOnly 5% and clusOnly 7%), which represents 12% of the misclassifications. The major part of the misclassified images are images with couplets missed by PRED BIST. The missed couplets and triplets are local defects that can be subject to discussion. In fact, a difference of few pixel values can be difficult to detect if the x parameter used to set up the envelope is not well chosen. Moreover, if the x parameter varies, one pixel of the couplet can toggle from correct to defective, or vice-versa. During the test, PRED BIST is able to find one of the defective pixel forming the couplet but may not find the other defective pixels of the couplet, so it classifies the defect as a simple singlet, unlike what would be done by an ATE-based optical test.

PRED BIST finds that 5% of the misclassified images have too many couplets compared to the couplets limit and 7% of the misclassified images have a cluster whereas the ATE-based optical tests do not find any issues inside the images (or find a number of couplets bellow the admissible couplets limit). After visually studying the misclassified images, the visual analysis allows us to classify them as *FAIL* due to some visible breaks in the uniformity. This means that the calibration of PRED BIST are stricter than the calibration of ATE-based optical tests. With PRED BIST calibration, it is possible to reach a higher accuracy compared to the tolerances currently accepted in production. In fact, the calibration of the optical tests performed with an ATE is chosen in order to let pass images with specific defects, considered as admissible.

An important defect type that should not be left behind by PRED BIST is a cluster. The visual study of the images (3% of the misclassifications as reported in Fig. 13) shows that the missed cluster corresponds to a local group of few defective pixels (*i.e.*, more than three defective pixels) with a slight difference of pixel values compared to the values inside the A*A kernel of pixels. No defective row or column, i.e., global defects, are missed by PRED BIST. This is an important information since it is not admissible to miss one or several global defects inside the image.

D. Results for DB2

PRED BIST has been used for the optical test of sensor providing images in DB2. The same process of compilation at several levels, presented in Section V.B for DB3, is done on the result data in DB2.

After all compilations, the correlation between results from ATE-based optical tests and those from the use of PRED BIST are 99.90% for 11,450 CISs. We identified that only 0.10% of the CISs are classified as *FAIL* by PRED BIST whereas the ATE-based optical tests have not identify any defect inside these CISs. By looking at the images from the 0.10% misclassification, local defects such as triplets are identified by PRED BIST. 100% of this misclassification comes from the clusOnly cause. More precisely, PRED BIST identifies triplets that are missed by the optical test performed with an ATE. We can conclude that for the chosen x parameter, PRED BIST is more accurate than the ATE-based optical tests regarding triplet detection.

VI. Discussion

The optical test performed thanks to an embedded test solution induces a trade-off between the cost (area overhead) of the BIST insertion inside the CIS under test and the reduction of the test time. PRED BIST takes approximately 1.5% of the total area of a 1.5 MegaPixels CIS (monocolor) whereas PETS BIST takes 0.25% of the total area of the same CIS. PRED BIST is bigger than PETS BIST as the complexity of the first one is higher than the second one. Indeed, PETS BIST uses 1D basic image processing algorithms while PRED BIST uses an arithmetic method based on a bilinear interpolation.

The architecture of PETS BIST highly depends on the CIS type (monocolor or RGB). If the CIS type is RGB, PETS BIST needs more accumulators (inside the *defective pixel and line detection* blocks) to sort pixels regarding their type, thus inducing additional storage resources (registers). Conversely,

the architecture of PRED BIST is less dependent to the type of the CIS under test because it does not need accumulators to sort the PUT regarding its type. This is due to the fact that PRED BIST performs a sequential operation (color image by color image) when PETS BIST operates in parallel on the color images. Moreover, if the number N used to encode the pixel value increases, the architectures of both BISTs will increase due to the addition of flip-flops.

The graph in Fig. 14 illustrates the two BIST solutions area overhead in percentage versus the total area for ten different monocolor CISs.

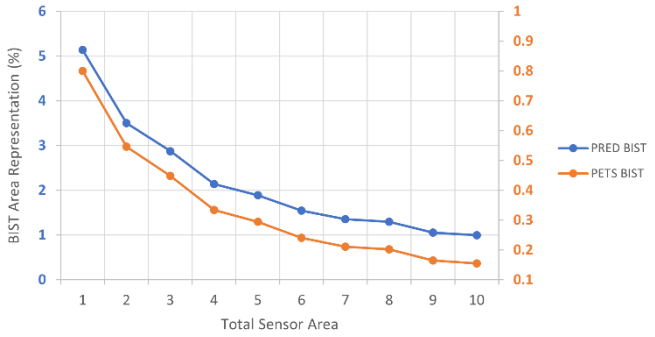

Figure 14: BIST area overhead representation in % versus the total sensor area for 10 different monocolor CISs (little CIS on the left and big CIS on the right)

The littlest CIS is on the left of the horizontal axis and the biggest one is on the right. The area of PETS BIST is represented in orange and the area of PRED BIST is represented in blue. We can notice that the BIST insertion is more interesting for the bigger CISs than for the little ones because the area of the BISTs represents less percentage for the bigger CISs. The trends of the two curves are similar but the gap between maximum and minimum percentages of the PRED BIST curve is bigger (4.14% of difference) than the one of PETS BIST (0.65% of difference).

In terms of defect detection, PETS BIST can cover 50% of the ATE-based optical tests but it misses global defects such as subtle defective column. So, it still needs an ATE to perform the global defect detection. A solution exists to detect the global defects, but it induces additional logic, thus increasing the area of the BIST, hence negatively impacting the cost-benefit aspect of PETS BIST. Conversely, PRED BIST does not need an ATE to perform optical tests and it covers 100% of the ATE-based optical tests, but it misses some local defects such as couplets or triplets. However, local defects being less critical than global defects, it will cost less to embed additional digital resources to perform local defect detection than to embed resources to perform global defect detection.

By using PETS BIST to perform the optical tests of DB2 CIS, a correlation of 99.64% is reached and 30% of the optical test time is saved when the usage of PRED BIST gives 99.40% correlation and 95% of the optical test time is saved. In fact, PRED BIST misses defects with low impact on the quality of the output images when PETS BIST misses critical defects which induce to reject the CIS.

VII. Conclusion

In this paper, we have presented a new BIST solution to perform all the optical tests during CIS testing. It is based on the creation of an ideal image to detect global and local defects inside the images from the CIS under test. The novelty of the approach relies on the ability to predict a ideal image from each output image of the CIS without the need to launch external optical tests performed with an ATE as for the PETS BIST solution presented in [1] and [2]. The detection of the global and local defects is used to define whether images are good or bad and, finally if the CIS need to be rejected or not. A software emulation of the PRED BIST engine has been done to validate the test solution. Experiments carried out on images coming from two DBs of different sensors (monocolor and RGB) have shown that our proposed solution adequately classify CIS into *PASS* and *FAIL* categories in 99.90% and 99.40% of cases. The simulation and synthesis of PRED BIST, designed in Verilog language, show that PRED BIST represents 1.5% of the total area of a 1.5 MegaPixels CIS and allows to reduce by 95% the optical test time.

References

[1] J. Lefevre, P. Debaud, P. Girard, and A. Virazel, "A Fast and Low-Cost Embedded Test Solution for CMOS Image Sensor", *in Proc. IEEE International Test Conference, 2021*, [IEEE_ITC2021_article].

[2] J. Lefevre, P. Debaud, P. Girard, and A. Virazel, "A Generic Fast and Low-Cost BIST Solution for CMOS Image Sensor", *in Proc. IEEE European Test Symposium, 2022*, [IEEE_ETS2022_article].

[3] B. Luo, F. Yang, and L. Yang, "Key Technologies and Research Development of CMOS Image Sensors", *in Proc. IITA International Conference on Geoscience and Remote Sensing*, 2010.

[4] R.Fei. "Alternative Solution to Improve the Production Test of Optical Sensors in CMOS Technology", PhD dissertation, Grenoble Alpes University, 2015.

[5] J. Chen, "CIS Testing Technology", Jetek Technology corporation, 2018. [CIS_testing_technology_article]

[6] Quality Testing Services, "Breakdown on Costs of Testing vs. Cost of Not Testing," May 1, 2019. [QualityTest_article]

[7] A. Grochowski, D. Bhattacharya, T.R. Viswanathan, K. Laker, "Integrated Circuit Testing for Quality Assurance in Manufacturing: History, Current Status, and Future Trends", *in Proc. IEEE Transactions on circuits and systems-II: analog and digital signal processing*, vol. 44, NO.8, 1997.

[8] I.L. Fujimori, "CMOS Passive Pixel Imager Design Techniques", PhD dissertation, Massachusetts Institute of Technology , 2002, [Active_Passive_Pixels_article].

[9] Leung, Jenny & Chapman, Glenn & Koren, Zahava & Koren, Israel. (2009). Statistical identification and analysis of defect development in digital imagers. 72500. 10.1117/12.806109 [ResearchGate_article].

[10] Standard Test Data Format (STDF) Specification, Version 4, Table of Contents, 2007, [SemiEngineering_article].

[11] M.B. Kaplinski, G. Waligorski, V. Berezin, and E.R. Fossum, "Test Methodologies for Digital CMOS Camera-on-a-Chip Image Sensors", *in Proc. IEEE Workshop on CCDs and Advanced Image Sensors*, pp. 239-241, 1999.

[12] C.C. Wan, "CMOS Image Sensors with Multi-Bucket Pixels for Computational Photography", PhD dissertation, Stanford University, 2011

[13] Advantest corporation, "CMOS Image Sensor Test Solution", 2017. [Advantest_slides]

[14] R. Fei, J. Moreau, S. Mir, A. Marcellin, C. Mandier, E. Huss, G. Palmigiani, P. Vitrou, and T. Droniou, "Horizontal-FPN Fault Coverage Improvement in Production Test of CMOS Imagers," *in Proc. IEEE VLSI Test Symposium*, pp. 1-6, 2015.

[15] Weisstein Eric W., "Gaussian Function", MathWorld--A Wolfram web Resource, [Wolfram_MathWorld_article]

[16] M. Tusch, G. Cooper, and T. Atherton, "Combining an ISP and Vision Processor to Implement Computer Vision", Embedded Vision Alliance, 2019, [Edge-ai-vision_article]

[17] J. Piard & C. Doré, & J-P. Placial, "Questioning the colors perception: an optical illusion with the bromophenol blue", ENS Cachan, experimental article, 2016, [ResearchGate_article].